

The effect of vibration and translational energy on the reaction dynamics of the $\text{H}_2^+ + \text{H}_2$ system

Scott L. Anderson,^{a)} F. A. Houle,^{b)} D. Gerlich,^{c)} and Y.T. Lee

Materials and Molecular Research Division of the Lawrence Berkeley Laboratory and Department of Chemistry, University of California, Berkeley, California 94720
(Received 30 March 1981; accepted 15 May 1981)

A new experimental technique combining molecular beams, photoionization, and guided beam ion optics has been used to study several isotopic $\text{H}_2^+ + \text{H}_2$ reactions. The technique is described. By using this method we are able to observe the effects of both reagent translational and vibrational energy. Cross sections are reported for charge transfer, H_3^+ formation, and collision induced dissociation. Evidence is seen for competition between the channels, charge hopping in the reaction entrance channel, potential energy surface hopping, reaction on excited potential surfaces, and isotopic scrambling. A model for the reaction which takes into account the multisurface nature of the systems seems to explain the results satisfactorily.

I. INTRODUCTION

The reaction $\text{H}_2^+ + \text{H}_2 \rightarrow \text{H}_3^+ + \text{H}$ has been extensively studied over the years. The interest in this reaction stems partly from its importance in interstellar¹ and atmospheric² chemistry, and partly because of its suitability for rigorous theoretical treatment. Experimentally it has been studied by crossed beam,³ mass spectrometric,⁴ merged beam,^{5,6} photoionization,⁷ ICR,⁸ and ion beam-gas cell⁹ techniques. The experiments have provided a reasonably clear picture of the gross reaction dynamics. The reaction is exoergic by 1.7 eV and, contrary to early speculation, appears to proceed almost entirely by a direct mechanism^{3,5} without any observable barrier.^{5,6} Studies of $(\text{H}_2)_2^+$ photoionization in our laboratory also indicate that H_4^+ is indeed unstable with respect to $\text{H}_3^+ + \text{H}$, demonstrating the lack of a barrier to reaction.¹⁰ The reaction cross section is very large ($\sim 100 \text{ \AA}^2$) at thermal energies, and falls off rapidly with increasing collision energy.^{5,6}

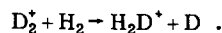
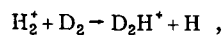
In the available experimental work, there are two observations that indicate the existence of complexities in this apparently simple reaction. In the $\text{H}_2^+ + \text{H}_2 \rightarrow \text{H}_3^+ + \text{H}$ reaction, H_3^+ may in principle, be formed by proton or H atom transfer mechanisms. The proton transfer involves breaking the H_2^+ bond ($D^\circ \approx 2.6 \text{ eV}$), while H atom transfer requires H_2 neutral bond rupture ($D^\circ \approx 4.5 \text{ eV}$). One might expect that the two channels would have very different dynamics, and in particular, that proton transfer would predominate. In trajectory calculations by Muckerman¹¹ it is found in fact, that only proton transfer occurs. Experimentally, by using isotopic substitution, it is found that products corresponding to both nominal H atom and proton transfer reactions occur with comparable cross sections and similar dynamics.^{3,5} This appears to be the consequence of extensive charge transfer between the reagents.^{3,5,11}

Secondly, in pioneering work by Chupka *et al.*,⁷ and

more recently by Koyano and Tanaka,¹² using photoionization to prepare vibrationally state selected H_2^+ , it is observed that at low collision energies ($E_{\text{c.m.}} < 1 \text{ eV}$), H_3^+ formation is inhibited by vibrational excitation of the H_2^+ reagent, and that at higher energies, there is some vibrational enhancement. These two aspects of the reaction have been linked to the interaction of several potential energy surfaces.^{3,13}

There have been a number of good calculations of the H_4^+ ground state potential energy surface (PES).¹⁴ These calculations show quite clearly the absence of a barrier for the $\text{H}_2^+ + \text{H}_2 \rightarrow \text{H}_3^+ + \text{H}$ reaction, thus supporting the experimental observation of direct reaction dynamics. If it exists at all, H_4^+ appears to be stable only as a weakly bound $\text{H}_3^+ \cdots \text{H}$ complex in the PES exit channel, but not as $\text{H}_2^+ \cdot \text{H}_2$. There have also been DIM (diatomics-in-molecules) calculations by Krenos *et al.*³ and Stine and Muckerman.¹³ This work shows that there is considerable interaction between the ground and excited PES's, and in particular there are a number of avoided crossings. These not only distort the ground state surface, but allow the possibility of repeated surface hoppings, opening up a number of excited pathways for reaction.

This set of interacting PES's allows an explanation of the above mentioned experimental observations. Consider two sets of $\text{H}_2^+ + \text{H}_2$ isotopic reagents, $\text{H}_2^+ + \text{D}_2$ and $\text{D}_2^+ + \text{H}_2$, which are just the two reagent charge states of the $(\text{H}_2 + \text{D}_2)^+$ system. Assuming that reaction is exclusively by proton transfer, different triatomic ions will be produced from the two sets of reagents:



At infinite reagent separation, the two reagent charge states are described by two different potential energy surfaces, which cross at points where the ion and neutral bond lengths are equal.^{3,14} As the reagents approach, however, the surface crossing becomes avoided, and the two sets of reagents correspond simply to two different entrance valleys on the ground PES. The barrier between the two decreases with decreasing reagent separation, until at $\sim 8-10$ bohr the barrier becomes smaller than the reagent zero point energy. At this point rapid interconversion (charge hopping) between

^{a)}National Science Foundation Graduate Fellow.

^{b)}Present address: IBM Research Laboratory, 5600 Cottle Road, San Jose, Cal. 95193; IBM Postdoctoral Research Fellow, 1979-80.

^{c)}Permanent address: Fakultät für Physik der Universität Freiburg, D-7800, Freiburg, West Germany.

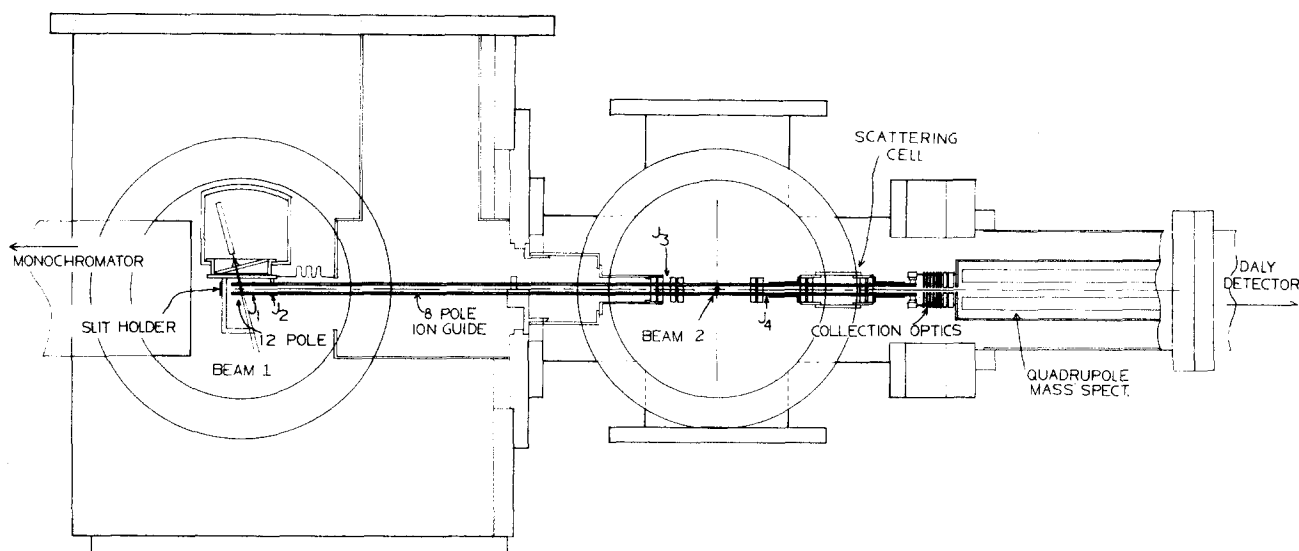


FIG. 1. Schematic of the apparatus.

$\text{H}_2^+ + \text{D}_2$ and $\text{D}_2^+ + \text{H}_2$ may occur. This would also allow production of both the D_2H^+ and H_2D^+ product ions from each set of reagents, explaining the experimental similarity of the nominal "atom" and "proton" transfer reactions. The charge hopping is induced by reagent vibration, and the mixing of the two reagent charge states might be expected to be somewhat dependent on reagent vibrational state.

Krenos *et al.*³ also suggested an explanation for the vibrational inhibition of the formation of H_3^+ at low collision energies. They suggest that reagent vibration promotes hopping of the system from the ground surface [$\text{H}_2^+(\Sigma_g) + \text{H}_2$] to the first excited surface [$\text{H}_2^+(\Sigma_u) + \text{H}_2$]. Since DIM calculations show a large barrier to reaction on the excited surface, this hopping decreases reaction probability.

It appears that due to the multiple surface nature of the H_3^+ system, the detailed reaction dynamics including reagent charge transfer and surface hopping are likely to be strongly influenced by reagent vibration. Unfortunately, in all existing experiments with the exception of the photoionization studies,^{7,11} the H_2^+ reagent is prepared using electron bombardment. This populates an approximately Franck-Condon distribution of vibrational states^{3,5,6} which ranges from $v=0$ up to the H_2^+ dissociation limit ($\sim v=16$), with a peak at $v=2$.¹⁵ Thus it is possible that the dynamics observed in the crossed³ and merged beam^{5,6} experiments may reflect greater involvement with all accessible potential energy surfaces than would occur for reagents in their ground vibrational state. In particular, charge exchange and the involvement of excited potential surfaces may be much more important.

Previous photoionization work by Chupka *et al.*⁷ and Koyano and Tanaka¹² has provided interesting data on vibrational effects in the $\text{H}_2^+ + \text{H}_2$ reaction over a kinetic energy range of 0–1 eV. Above ~ 1 eV experimental complications in the use of a single chamber for ion production and reaction have allowed only qualitative

data to be obtained. Also, their single chamber arrangement makes it difficult to use isotopic substitution to distinguish between different initial reagent charge states leading to the same products (e.g., D_2H^+ from $\text{H}_2^+ + \text{D}_2$ and $\text{D}_2^+ + \text{H}_2$). It would be especially desirable to extend the measurement of the effects of reagent vibration and collision energy on other channels, and inter-channel branching ratios for various isotopic systems. This detailed mapping of the reaction vibrational and translational energy dependence certainly would yield some dynamical insight, and in particular, would provide a very sensitive test of any theoretical modeling of the scattering of $\text{H}_2^+ + \text{H}_2$.

We have recently completed construction of an apparatus which allows the study of the vibrational and translational energy dependence of ion molecule reaction cross sections at high resolution. Since $\text{H}_2^+ + \text{H}_2$ is an ideal system, we have elected to start with it. This paper reports the design of our apparatus and our results on triatomic ion production, charge exchange and collision induced dissociation in the H_3^+ system.

II. EXPERIMENTAL

A schematic of the apparatus, which consists of a photoionization source, radio frequency beam guide ion optics, and an ion detector, is shown in Fig. 1.

In order to control the internal energy of a reagent ion, ions are formed by photoionization. In general, photoionization allows control of the maximum internal energy of the ion. In many cases (e.g., NO, NH_3 , Ar)¹⁶ it is possible to prepare ions with well characterized distributions of internal states, and to study the reactions of individual states by difference techniques. The best case is H_2 photoionization, where it is possible to prepare single vibrational states with high purity. This is possible because the H_2 photoionization is dominated by very strong vibrational autoionization, with little direct ionization as shown by Dehmer and Chupka.¹⁷

The source of vacuum UV photons is a 9 in. capillary discharge lamp. Depending on the photon wavelength desired, we use either a dc discharge in H_2 (900–1650 Å), or in the present case, a pulsed discharge in helium (700–900 Å). The wavelength is selected by a 1 m near-normal incidence monochromator (McPherson 225) set to 4 Å resolution. The light beam emerges from the collimating slit of the monochromator, and passes into the ionization chamber.

The neutral hydrogen molecules are formed into a molecular beam, collimated, and passed through the ionization chamber. The photon and molecular beams intersect inside the ion guide in a volume roughly 2 mm in diameter and 1 cm high. The use of a molecular beam to create a small volume of high density ($>10^{-4}$ Torr) gas in a chamber evacuated to $\sim 10^{-7}$ Torr is essential—this avoids extensive ion-molecule reaction in the ion source. In addition, the ions produced are translationally cold. The molecular beam is tilted 15° from the vertical to allow the ions to be more easily formed into a beam along the direction of the ion guide. The combination of molecular beams and photoionization is an exceptionally clean but inefficient ion source, due to limited photon intensity. Typically ion beam intensities are less than 2×10^4 ions/s. In order to efficiently use the ions, and maintain a narrow translational energy spread, we have employed the guided beam method¹⁸ of Teloy and Gerlich. The ion guides are constructed of eight 1/8 in. molybdenum rods, symmetrically spaced around the circumference of a 1 in. diameter cylinder. Alternate poles (or rods) are connected to opposite phases of an rf oscillator circuit (30 MHz). The effect is to set up a cylindrically symmetric effective potential which confines the ions to the inner ~ 1 cm of the guide. The effective potential of the octopole field is of the form

$$V_{\text{eff}} = \frac{e^2 V_0^2}{4m\omega^2 R_0^2} \left(\frac{R}{R_0}\right)^8,$$

where V_0 and ω are the peak voltage and frequency of the rf, R is the distance from the octopole axis, R_0 is the radius of the octopole (0.5 in.), and m is the mass of the ion. This effective potential has very steep repulsive walls, close to the ideal case, a square well. Thus the rf trap behaves as an ion guide or pipe. The guided beam technique is slightly more difficult to construct than conventional dc ion optics, but it has several major advantages. The most important of these is that none of the ions formed are lost in transit from source to reaction chamber. It is possible to achieve 100% transmission without resorting to typical accelerating ion lens systems which tend to destroy the ion beam energy resolution. Our beam spread, measured by time of flight, is smaller than 50 meV. Another advantage is that the octopoles effectively shield low energy ions from stray fields, and to some extent reduce sensitivity of the beam to contact potentials. Evidence for this is that an ion beam can be generated at energies down to a few tenths of an electron volt. Furthermore, the beam energy has been found to drift only ~ 200 meV over several months of continuous operation. The ion guide is broken into segments at joints

(J_1), to allow control of the ion translational energy by application of independent dc potentials to each segment. To avoid problems with injecting ions into the guide, the ions are formed inside the first segment of the guide. Since the vertical exit slit of the monochromator results in a oblong ionization volume, this first segment has been expanded by addition of 4 poles to produce an oval 12-pole geometry. This insures that the ions will all be produced in the field-free center of the ion guide. The next segment is shaped and dc-biased in order to form the ions into a beam, collinear to the guide axis. It also transforms the guide to the normal cylindrical 8-pole geometry. In the third long guide segment the ions pass through a differential pumping wall, enter the reaction chamber, and are accelerated to the desired collision energy at J_3 .

Ion-molecule reactions can be carried out in two modes. For high collision energy resolution, experiments can be performed by passing a supersonic molecular beam of the neutral reactant through the octopole (beam source 2). Because of the narrow angular and translational energy spread of the neutral beam, the collision energy spread under these conditions is almost entirely due to the energy spread (<50 meV) and transverse velocity component of the ion beam. The equivalent spread of transverse energy is only ~ 10 meV, thus the high resolution arrangement gives approximately 60 meV FWHM laboratory collision energy spread. The signal intensity is extremely low (<1 cps), and measurements lasting several hundred hours are required.

Lower resolution experiments can be carried out by guiding the ion beam through a scattering cell, which is the experimental arrangement used for the data reported here. Gas pressures are kept low enough to ensure that at most $\sim 5\%$ of the ion beam reacts. Beam-gas experiments have inherently lower kinetic energy resolution because of the thermal motion of the target gas. The resolution when the ion beam energy spread is negligible has been shown to be¹⁹

$$\Delta E_{\text{FWHM}} = [11.1(m/M+m) kT E_{\text{c.m.}}]^{1/2},$$

where m is the ion mass, M is the mass of the target gas, and $E_{\text{c.m.}}$ is the nominal center-of-mass collision energy. Because the ion guides are heated to maintain cleanliness, the target gas temperature is $\sim 400^\circ\text{K}$. At this temperature, the kinetic energy spread for $\text{H}_2^+ + \text{D}_2$ is $(0.13 E_{\text{c.m.}})^{1/2}$ eV.

In either the beam-beam or beam-gas modes, all reactions occur inside the ion guide, ensuring confinement of all product ions. The effective potential and dc bias of the ion guide prevents escape of the ions in any direction except toward the detector. Thus the beam guides guarantee total product collection, regardless of collision energy, reaction dynamics, vibrational states, etc. This eliminates one of the most serious sources of dynamical bias in product detection that is common in this type of experiment, especially at low laboratory energies.

At the exit from the octopole, conventional electrostatic lenses extract the ions, accelerate them to 70 eV, and inject them into a quadrupole mass filter, which

TABLE I. Estimated vibrational distributions.

Estimated vibrational distribution	H_2^+ v nominal					D_2^+ v nominal				
	0	1	2	3	4	0	1	2	3	4
0	1	0.11	0.08	0.08	0.07	1	0.10	0.06	0.06	0.4
1		0.89	0.16	0.17	0.14		0.90	0.14	0.13	0.10
2			0.76	0.19	0.16			0.80	0.20	0.15
3				0.56	0.15				0.61	0.17
4					0.48					0.55

selects the ion of interest. Transmission losses are quite small as can be assessed by observation of a negligible increase in ion signal when the mass spectrometer is switched from the primary ion mass to the nonmass selective mode. After mass selection, the ions are counted by a Daly detector.²⁰ This consists of a negative high voltage target which emits electrons on ion impact, and a scintillator-PMT combination which detects the electrons repelled from the ion target. Measurements of detection efficiency versus target voltage were carried out for all the ion masses in this experiment. It was found that the efficiency saturated for all masses at ion target voltages larger than 40 kV. This is assumed to be near unit detection efficiency. All experiments were performed at this voltage.

The data presented here have been obtained under computer control in two different modes. In one of these, the ionizing photon wavelength is kept fixed while the ion kinetic energy is varied, typically from 0–10 eV in 0.1 eV steps. The other mode involves scanning the monochromator at fixed ion kinetic energy. The wavelength step size is chosen such that the same set of wavelengths is used in both the variable energy and variable wavelength experiments. It is for those photon energies that vibrational distributions of H_2^+ have been estimated, as will be described later. In both modes cross sections are determined in the following manner. Since the scattering cell is not sealed, gas leakage establishes a constant background pressure of the neutral reagent throughout the reaction chamber, allowing some reactions to take place outside the scattering cell. This background signal is corrected for by measuring product ion intensities first with the scattering cell pressurized to $\sim 10^{-4}$ Torr, as measured by a Baratron capacitance manometer, the resulting background pressure being $\sim 2 \times 10^{-6}$ Torr; then with the scattering cell empty and the reaction chamber filled to the same background pressure. Subtraction of the two measurements gives the product ion intensity resulting from reactions in the scattering cell itself (S). Measurement of the unattenuated primary beam intensity I_0 , the target gas density n , and knowledge of the length of the scattering cell L allow calculation of the absolute reaction cross section according to the relation $\sigma = (S)/(I_0 n L)$. Ion intensities as a function of energy or wavelength are scanned repetitively until the desired signal to noise ratio is obtained. Typical experiments last 8–15 h each.

The cross sections from both types of measurements are compared, and usually agree to within $\pm 5\%$. Having

both types of information allows correction for any small systematic errors, and identification of bad data. Thus it is possible to obtain cross sections accurate in both their collision energy and wavelength (vibrational state) dependence.

These data can then be deconvoluted using the vibrational state distribution generated at each ionization energy in order to obtain cross sections as a function of pure vibrational state. The relevant distributions can be obtained for many molecules by analysis of step structure in their photoionization spectra combined with Franck–Condon factors from photoelectron spectroscopy. However, for H_2 , because of the domination of autoionization near the threshold, it is possible to estimate the state distribution for H_2^+ from high resolution photoionization spectra of H_2 . In H_2 autoionization, ionization occurs, where possible, by a $\Delta v = 1$ process, and even when autoionization is only possible by a $\Delta v > 1$ process, the ions are still formed predominately ($> 75\%$) in the highest possible vibrational state.²¹ Thus, tuning the photon energy to excite states which are between the $H_2^+(v=n)$ and $H_2^+(v=n+1)$ ionization limits produces mainly H_2^+ in the $v=n$ state. To obtain the actual H_2^+ vibrational distributions as a function of photon energy it is necessary to take into account both autoionization and direct ionization contributions. The very high resolution H_2^+ spectrum¹⁷ of Dehmer and Chupka was used to estimate the ratio of direct to autoionization at the photon energies used for H_2^+ production. Franck–Condon factors obtained by photoelectron spectroscopy¹⁵ provide an estimate of the vibrational state distributions from direct ionization. These are combined with the autoionization contribution (assumed to yield the highest possible v state), to obtain the distributions shown in Table I. The same procedure was used for D_2 , except that since no high resolution photoionization spectra have appeared for it in the literature, the direct/autoionization ratios determined for H_2 were used.

The rotational distribution of the ions is not selected. It consists of $J = 0$ to 4, and with our photon band width, the distribution cannot vary significantly from vibrational state to vibrational state. Chupka⁷ has shown that any rotational effects on the reaction cross sections for $H_2^+ + H_2$ are small ($< 10\%$).

There are several sources of error which could affect the accuracy of the absolute cross sections reported here. The uncertainty in the gas pressure distribution along the length of the scattering cell and in

the pressure measurement, limits the absolute accuracy to $\sim \pm 25\%$. Nevertheless, our data are in good agreement with those from other sources.^{5,7,12} Reproducibility of the data is very high (within 5%) and thus the relative error in the present work is actually much lower than the absolute error. A less quantifiable error is introduced by the vibrational state distributions listed in Table I. The values are best estimates only, and since they are used to subtract reaction contributions from lower states from the cross sections obtained for higher states, any errors present are propagated through the whole data set. However, the relatively high vibrational state purity at each wavelength (ranging from 100 to 50%) tends to minimize the effect of such a propagation. Furthermore, all of the variations in reaction cross sections with vibrational state were evident in the raw data, and merely enhanced by the unfolding procedure.

III. RESULTS

Several processes are possible in the $H_2^+ + H_2$ system: H_3^+ formation, collision-induced dissociation, and charge transfer. Although the present experiments focus on the reactive channel, limited data were also obtained for the collision-induced dissociation and charge transfer channels in order to investigate competition between these processes.

A. Triatomic ion production

Cross sections have been measured for the reactions:



The other reaction product, DH_2^+ can not be distinguished mass spectrometrically from D_2H^+ which is the charge transfer product in $H_2^+ + D_2$ and the reagent in $D_2^+ + H_2$. In both cases the collision energy was varied from

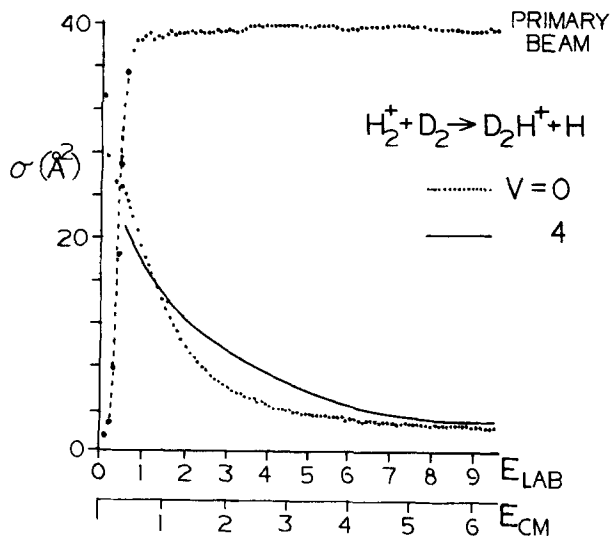


FIG. 2. Typical quality data. Upper trace is the transition function of the primary ions. The two lower traces are cross sections for D_2H^+ formation from H_2^+ ($v=0, 4$) + D_2 .

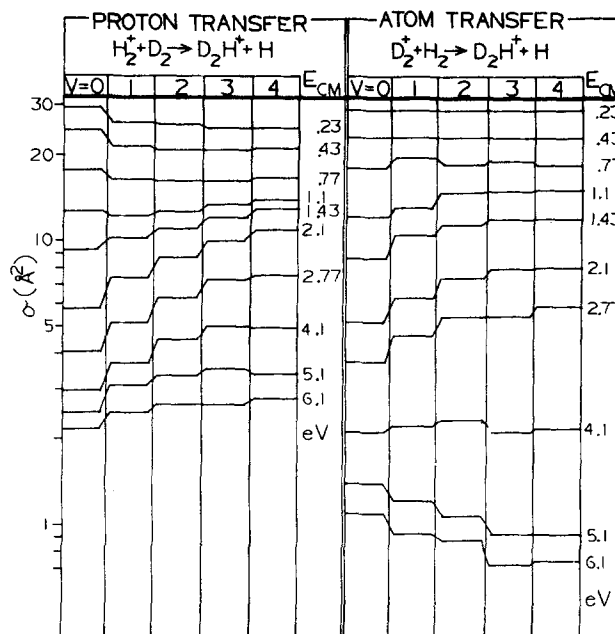


FIG. 3. Vibrational and translational energy dependence of D_2H^+ formation reactions.

$E_{c.m.} = 0$ to 6 eV, and the ion vibrational state from $v=0$ to 4. A typical example of raw data for Reaction (1) is shown in Fig. 2. The cross section falls rapidly with collision energy, as expected for an exoergic ion-molecule reaction. Since all the cross sections measured for Reactions (1) and (2) have the same gross shape, they have been plotted in Fig. 3 in a way that emphasizes the effects of reagent vibration. For selected collision energies (right margins), cross sections for ion vibrational states 0–4 are compared for Reactions (1) and (2). Results of both wavelength and kinetic energy scans were used to obtain these data.

For $H_2^+ + D_2 \rightarrow D_2H^+ + H$, the nominal proton transfer reaction, vibrational energy inhibits reaction at low collision energy, but enhances it at energies above ~ 1.4 eV. For the $D_2^+ + H_2 \rightarrow D_2H^+ + H$ atom transfer reaction there is essentially no vibrational effect at low energies, substantial vibrational enhancement from $E_{c.m.} \approx 1$ to 3 eV, and a sharp, vibrational energy dependent fall off at energies greater than 3 eV.

The earlier observations^{7,12} of vibrational inhibition of the $H_2^+ + H_2 \rightarrow H_3^+ + H$ reaction at low collision energy are compatible with the sum of the proton transfer and atom transfer reactions, since both lead to H_3^+ product. Here proton and atom transfer are being used only as labels for the two reactions, and do not imply anything about the microscopic dynamics of the reactions.

At a given $E_{c.m.}$, the relative error in the cross sections for different vibrational states ranges from $\sim \pm 0.5 \text{ \AA}^2$ at low $E_{c.m.}$ to $\sim \pm 0.25 \text{ \AA}^2$ at the highest $E_{c.m.}$. Since the cross sections fall quite rapidly with increasing $E_{c.m.}$, this decrease in absolute error actually constitutes an increase in percent error. Thus, for example, the oscillatory behavior for the atom transfer channel at 0.77 eV is real, while that at 4.1

eV probably is not. The relationship of the data at different values of $E_{\text{c.m.}}$, was taken from scans of $E_{\text{c.m.}}$ for fixed vibrational states. This error is also $\sim \pm 0.25 \text{ \AA}^2$, except at the very lowest energy, where problems with transmission of the slow primary and product ions may cause errors as large as $\pm 1.5 \text{ \AA}^2$. Relative error in comparison of the two sets of internally consistent data for Reactions (1) and (2), arises from the difference in the ratio of reagent ion mass to target mass. This introduces a possibility of error in defining the zero of the CM energy scale for Reactions (1) and (2), which in turn introduces an error in comparing cross sections at a given $E_{\text{c.m.}}$. Due to the shape of the cross section, this effect is worst at low $E_{\text{c.m.}}$ ($\pm 1.5 \text{ \AA}^2$), and is negligible at energies above $\sim 2 \text{ eV}$.

B. Collision induced dissociation (CID)

Because of possible interplay between CID and the chemical reaction channels at higher collision energies, we have studied the effects of vibrational and collision energy on CID in $\text{D}_2^+ + \text{HD}$. This isotopic combination was chosen so that dissociation of the primary ion and the dissociation of secondary ions formed by charge exchange could be distinguished. Figures 4 and 5 show the cross sections obtained for D^+ and H^+ production. The thresholds shift to lower energy with increasing vibrational state, as expected, and there is sharp rise from threshold, followed by a leveling off at $E_{\text{c.m.}} \sim 5 \text{ eV}$. The thresholds are consistent with the dissociation energy of D_2^+ (2.69 eV) when consideration is made of the broadening in the $E_{\text{c.m.}}$ distribution induced by target gas motion. The curves shown result from averaging of the raw data, which was taken at 0.1 eV laboratory energy intervals, and subtraction of a small background signal which results from reactions of hot ions created by photoelectron bombardment in the ion source. The magnitude of this background corresponds to a

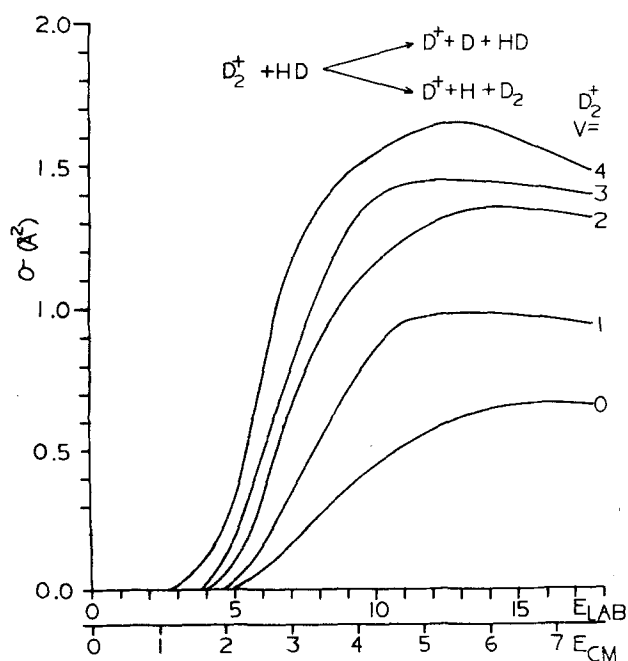


FIG. 4. D^+ formation cross sections from $\text{D}_2^+(v) + \text{HD}$.

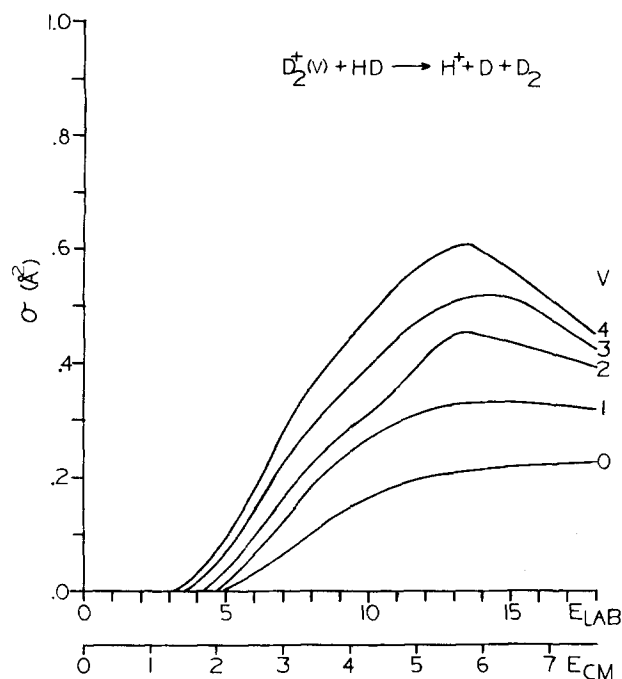


FIG. 5. H^+ formation cross sections from $\text{D}_2^+ + \text{HD}$.

cross section of 0.15 \AA^2 and that is also the magnitude of the estimated probable relative error.

Figure 6 shows the ratio of the D^+ production to the H^+ production. Although there are large variations in the ratio as a function of D_2^+ reagent vibrational state at low energies, for energies above 5 eV, where the cross sections level off, the ratio is 3 within experimental error. This is just the ratio of D atoms to H atoms in the reagents. We have also measured cross sections for CID of $\text{H}_2^+ + \text{D}_2$. Here we can only measure the H^+ production channel since D^+ cannot be distinguished from H_2^+ . It is interesting to note that the H^+ production cross sections have a magnitude which is $2/3$ that of the D^+ production cross sections in $\text{D}_2^+ + \text{HD}$. This suggests that CID is relatively free of isotope effects at high energy, and that the various isotopic ions are produced with equal probability. Our results are at variance with those of Futrell *et al.*²² who failed to observe H^+ production in CID of $\text{D}_2^+ + \text{HD}$.

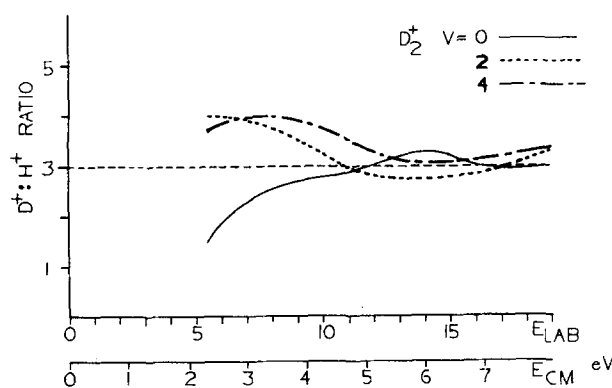


FIG. 6. $\text{D}^+ : \text{H}^+$ ratio in CID of $\text{D}_2^+ + \text{HD}$.

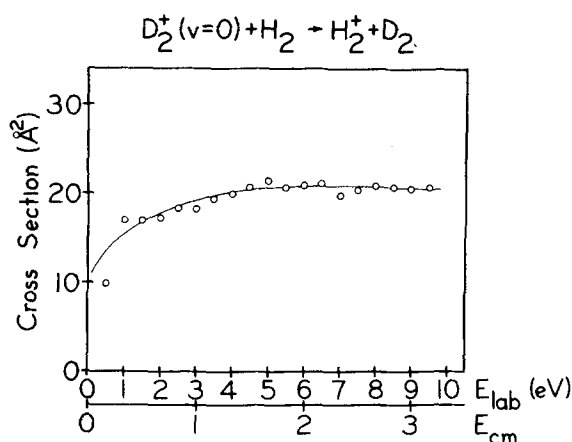


FIG. 7. $D_2^+(v=0) + H_2$ charge transfer cross section.

C. Charge transfer (CT)

Figure 7 shows our measured cross section for the reaction $D_2^+(v=0) + H_2 \rightarrow D_2 + H_2^+$. The cross section is large, and relatively independent of collision energy, except at very low energies. CT cross sections are difficult to measure in this experimental arrangement because the H_2^+ product ions are produced with little laboratory kinetic energy. These slow ions can then react with the H_2 in the scattering cell to form H_3^+ . In principle one can obtain the correct charge transfer cross section by merely adding the mass 2 and mass 3 production cross sections. In practice there are two additional problems. One is the contamination of the D_2^+ ion beam with approximately 2% HD^+ . Because our charge transfer cross sections are sensitive only to the net change in the mass 2 plus mass 3 ion intensity when the scattering cell is filled, only the reaction $HD^+ + H_2 \rightarrow DH_2^+ + H$ has an effect (negative) on the cross section. Since the HD^+ is only 2% of the reagent beam, and reagent ion attenuation is only 5%, and only one of the three major $HD^+ + H_2$ reactions has any net effect, the error introduced is small and we have not made any corrections for it.

A more serious problem is that some of the scattering gas (H_2) diffuses back into the ionization chamber and contaminates the D_2^+ beam with $\sim 4\%$ H_2^+ . Since reactions of H_2^+ with H_2 only yield mass 2 and 3, and the CT cross section is only sensitive to net change in m/e 2 and 3 signal when the scattering cell is filled. This component would have no effect on the measured CT cross sections as long as there is no change in the H_2^+ primary ion intensity when the scattering cell is filled. Unfortunately, filling the cell sends an effusive beam of H_2 into the ionizer. Because of the large separation (~ 50 cm) between the scattering cell and the ionizer, this only increases the H_2^+ intensity by $\sim 3\%$ (of 4%). We have corrected for this small but significant artifact by turning off the D_2 molecular beam and measuring the H_2^+ production and attenuation cross sections, which are then subtracted from the $D_2^+ + H_2$ CT cross section. Because this procedure is very time consuming, we have only carefully measured the CT cross section for D_2^+ $v=0$. However, comparison of uncorrected cross sections indicates little effect of reagent ion vibration

on $D_2^+ + H_2$ charge transfer. Similar behavior is seen in $H_2^+ + D_2$ CT.

IV. DISCUSSION

One of the most interesting features of the D_2H^+ production cross sections (Fig. 3) in reaction of $H_2^+ + D_2$ and $D_2^+ + H_2$ is the similarity between them. At low collision energy, the magnitudes of the proton and atom transfer reactions are very similar. Even more striking is the similarity of the pronounced vibrational effects in the energy range around 2 eV, which suggests that the two reactions may proceed through a common mechanism. This result is certainly consistent with the idea of rapid charge hopping in the reaction entrance channel,^{3,13} which was discussed in the introduction. Reaction then proceeds via proton transfer,¹¹ producing either $D_2H^+ + H$, or $DH_2^+ + D$, depending on the reagent charge state at the time of reaction. It appears that this charge hopping is quite facile, even for ground vibrational state reagents. The idea of efficient, long range charge hopping is certainly supported by the large, translational energy independent cross section for $D_2^+(v=0) + H_2$ charge transfer (Fig. 7). The 20 \AA^2 cross section implies an average range for the CT process of $\sim 2.5 \text{ \AA}$ if we allow for the possibility of multiple charge hops. This behavior is in good agreement with the calculations of Krenos *et al.*³ which show that charge hopping becomes likely at reagent separations $\sim 4 \text{ \AA}$. A prediction of Stine and Muckerman¹³ that net CT of ground vibrational state reagents would be unlikely due to competition with the reactive channel appears to be correct only at collision energies below 0.2 eV. The decrease in CT cross section at low collision energies, which we see for all reagent ion vibrational states, is almost certainly due to this competition, but the competition is not sufficient to eliminate CT altogether.

Although our data indicate extensive interconversion between the $H_2^+ + D_2$ and $D_2^+ + H_2$ charge states, there remain differences in the production of D_2H^+ from them. At very low collision energy, the reaction $H_2^+ + D_2 \rightarrow D_2H^+ + H$ shows vibrational inhibition, while on the other hand D_2H^+ formation from $D_2^+ + H_2$, which has a similar cross section, shows no vibrational effect. In $H_2^+ + H_2 \rightarrow H_3^+ + H$, the reaction is suppressed by vibrational energy at low collision energy.^{7,12} Krenos *et al.*³ suggested that the inhibition results from a vibrationally enhanced probability of hopping to the first excited PES. Since there is a barrier to reaction on this excited PES, collisions on it are nonreactive at low collision energies, and thus vibrationally enhanced surface hopping would lead to vibrational inhibition of the reaction at low collision energies. This vibrationally enhanced surface hopping would be expected to result in vibrational inhibition of both the $H_2^+ + D_2$ and $D_2^+ + H_2 \rightarrow D_2H^+ + H$ reactions. In order to explain the observed vibrational pattern, other effects must be considered.

$H_2^+ + D_2$ forms D_2H^+ simply by proton transfer. But the formation of D_2H^+ from $D_2^+ + H_2$, at least at low energies when other reaction mechanisms are inefficient, must proceed by a charge-transfer proton-transfer mechanism. Since charge hopping between the two reagent

charge states is vibrationally induced,^{3,14} one might expect that the $H_2^+ + D_2 \rightarrow D_2H^+ + H$ reaction would show vibrational inhibition with concomitant vibrational enhancement of H_2D^+ production, while $D_2^+ + H_2 \rightarrow D_2H^+ + H$ would be vibrationally enhanced at the expense of the H_2D^+ channel. The similarity in magnitude of the low energy reaction cross sections for the $H_2^+ + D_2$ and $D_2^+ + H_2$ charge states suggests that this charge transfer is very efficient at mixing the reagent charge states. This would result in there being only a small residual vibrational inhibition in D_2H^+ formation from $H_2^+ + D_2$ and a small enhancement for $D_2^+ + H_2$. Combining these two possible effects may explain the observed behavior. The reaction $H_2^+ + D_2 \rightarrow D_2H^+ + H$ is vibrationally inhibited by both surface hopping and charge transfer resulting in appreciable net vibrational inhibition. The $D_2^+ + H_2 \rightarrow D_2H^+ + H$ reaction on the other hand, is vibrationally inhibited by surface hopping and vibrationally enhanced by charge transfer. If the magnitudes of the two opposing effects are similar, they would cancel and no vibrational effect would be observed.

Hopping to an upper PES may also explain why both reactions show a strong vibrational enhancement in the intermediate collision energy range (1 to 3 eV). It may be that the system hops to the first excited PES as discussed above, but now has sufficient collision energy to surmount the barrier to reaction on the upper surface. If the excited PES reaction mechanism is *more* efficient than the ground state reaction, then we would expect to see net vibrational enhancement. If this mechanism is responsible for the observed enhancement, our data would yield a value of ~ 1 eV for the barrier.

As the collision energy increases above 1 eV the magnitude of the cross section of $D_2^+ + H_2 \rightarrow D_2H^+ + H$ (atom transfer) reaction begins to drop below that of the $H_2^+ + D_2 \rightarrow D_2H^+ + H$ (proton transfer) reaction, as shown in Fig. 3. Up to about $E_{c.m.} = 3$ eV the translational energy dependence and vibrational effects are very similar for both the proton and atom transfer cross sections, with simply a slow decrease in the relative magnitude of the atom transfer cross section. Above $E_{c.m.} = 3$ eV the decrease in relative cross section of the $D_2^+ + H_2 \rightarrow D_2H^+ + H$ (atom transfer) reaction becomes much faster. Then at $E_{c.m.} \sim 5$ eV the fall off stabilizes. Over this same energy range, the vibrational effect on the atom transfer reaction changes from enhancement to strong inhibition, while for the $H_2^+ + D_2$ (proton transfer) reaction the enhancement is only weakened.

It seems likely that the initial slow fall off of the $D_2^+ + H_2 \rightarrow D_2H^+ + H$ cross section relative to the $H_2^+ + D_2$ reaction is due simply to a breakdown of the entrance channel charge hopping which effectively mixes the two reagent charge states at low energy. Since proton transfer appears to be the dominant reaction mechanism at least at low collision energies, this breakdown would decrease the amount of D_2H^+ formed from $D_2^+ + H_2$ reagents. The fact that the CT cross sections (Fig. 7) remain large at high collision energies suggests that the breakdown of efficient charge hopping occurs only for the small impact parameter collisions which lead to reactive scattering.

While this breakdown mechanism is no doubt partly responsible for the large difference between the $H_2^+ + D_2 \rightarrow D_2H^+ + H$ and $D_2^+ + H_2 \rightarrow D_2H^+ + H$ reactions at energies above 3 eV, there seems to be another effect which is important. From $E_{c.m.} = 3$ to 5 eV, the $D_2^+ + H_2 \rightarrow D_2H^+ + H$ cross sections show a pronounced, vibrationally enhanced fall off. This fall off then stabilizes at energies above 5 eV. This general shape is very similar to what is observed for the CID cross sections for $D_2^+ + HD$ (Figs. 4 and 5). This strongly suggests that competition between D_2H^+ product formation and CID is occurring. Over the same energy range the $H_2^+ + D_2 \rightarrow D_2H^+ + H$ reaction cross section also shows a decrease in the degree of vibrational enhancement, some competition with CID is again suggested in this case.

Durup and Durup²³ have studied CID of $D_2^+ + D_2$, and suggested that CID occurs through a long lived intermediate. Our results on CID of $D_2^+ + HD$ and $H_2^+ + D_2$ show that in all cases CID is strongly vibrationally enhanced. Also, comparison of the results of H^+ and D^+ formation from $D_2^+ + HD$ and H^+ formation from $H_2^+ + D_2$ yields two important observations. First, of the four hydrogen (deuterium) atoms in the reactants, each one is equally likely to emerge as the detected proton (deuteron) at higher collision energies. This is shown for $D_2^+ + HD$ in Fig. 6. For $E_{c.m.}$ below 5 eV, the ratio depends strongly on the reagent ion vibrational state, while above 5 eV, the $D^+ : H^+$ ratio is just 3 ± 0.5 , for all D_2^+ reagent vibrational states. This is just the D atom : H atom ratio in the reagents. In addition, H^+ production cross sections in CID of $H_2^+ + D_2$ are very similar in shape to those for $D_2^+ + HD$ and the magnitudes are just 2/3 those for D^+ production from $D_2^+ + HD$ which is again the ratio of H atoms in the two systems. This suggests that, at least at high collision energies, CID proceeds by a mechanism in which the reagent mass ratio is unimportant, and which randomizes the outcome of the dissociation. This certainly suggests that CID proceeds through some sort of intermediate, in which all four atoms involved become equivalent.

There are a number of possible mechanisms for the isotopic scrambling which is observed in our CID results. One possibility is that during those $D_2^+ + HD$ collisions which eventually lead to CID, a fleeting D_3H^+ species is formed which lives long enough for isotopic scrambling to occur. Isotopic scrambling in the D_3H^+ could occur either by nuclear motion or by an electronic rearrangement in which all four atoms and bonds become equivalent. Another mechanism involves reaction to form a triatomic (D_2H^+ , D_3^+) product, which is internally excited enough to unimolecularly decompose, yielding net CID. Other mechanisms such as direct dissociation of the D_2^+ primary ion are hard to reconcile with both our and Durup and Durup's results.

For collision energies below 5 eV, the $D^+ : H^+$ production ratio in CID of $D_2^+ + H_2$ varies widely from the high energy value of 3. The variation is smooth with collision energy, but is very strongly dependent on D_2^+ reagent vibrational state (Fig. 6). This suggests that at collision energies near the CID threshold, kinematic effects involving different isotopes and the variation in

entrance channel charge hopping with reagent vibrational state might be important. For example, if charge hopping between $D_2^+(v=0) + HD$ is not efficient at small impact parameter, HD_2^+ will be the dominant product species, and further decomposition of some of the excited HD_2^+ will give a D^+/H^+ ratio of less than 3. On the other hand for D_2^+ in higher vibrationally excited states, charge hopping might be facile and produce excited D_3^+ and HD_2^+ intermediates in a statistical ratio. But because of the mass ratio, D_3^+ is likely to contain higher excitation energy and a larger fraction of D_3^+ could dissociate and give a D^+/H^+ ratio of greater than 3.

In any case, it is possible that at least part of the observed CID occurs through triatomic product decomposition, and thus competition between CID and D_2H^+ formation is not unreasonable. At high collision energies, both channels have similar magnitude cross sections, and both involve substantial rearrangement of the collision partners.

Examination of Fig. 3 shows that while the formation of D_2H^+ product from both the $H_2^+ + D_2$ and $D_2^+ + H_2$ reagents is suppressed by reagent vibrational and collision energy to some extent, the effect is much more dramatic for the $D_2^+ + H_2 \rightarrow D_2H^+ + H$ (atom transfer) reaction. Part of this is no doubt due to the fact that the cross section for atom transfer is smaller than that for proton transfer, and thus appears to be more strongly effected by the competition with CID. The size of the differences in cross sections and vibrational effects between the two reactions suggest however, that if competition between D_2H^+ formation and CID is the primary effect responsible for the differences, then D_2H^+ formed from $D_2^+ + H_2$ reagents must dissociate more than that formed from $H_2^+ + D_2$. This suggests that D_2H^+ product is formed with different degrees of internal excitation depending on the starting reagents. This could be a kinematic effect. But since kinematic effects do not seem to be very important in CID, it seems more likely that at $E_{c.m.}$ greater than ~ 3 eV the $D_2^+ + H_2 \rightarrow D_2H^+ + H$ reaction proceeds, at least in part, by a mechanism other than the low energy, charge exchange-proton transfer process. This second, high energy mechanism yields more excited D_2H^+ product which then dissociates with higher probability than D_2H^+ formed by proton transfer from $H_2^+ + D_2$ reagents. This high energy mechanism could include atom transfer or a number of excited PES reaction paths. If this is true, then if one could measure the H_2D^+ product cross sections from $H_2^+ + D_2$ and $D_2^+ + H_2$, the large depletion of product formation at collision energies above 3 eV, should appear in the $H_2^+ + D_2 \rightarrow H_2D^+ + D$ reaction.

V. CONCLUSION

Examination of the data presented here with previous work on the H_4^+ system has provided new information and new insights into the detailed dynamics of this "simple" chemical system. The present results add to the evidence for a direct mechanism for triatomic (H_3^+) ion formation. Extensive long range charge transfer is seen to be important. Evidence for both adiabatic and diabatic reactions has been discussed. A model for the

reaction, which takes into account the multi-PES nature of the problem as well as competition between different reactive channels, seems to explain the experimental results satisfactorily.

We have also shown that in contrast to neutral reactions where reagent vibration appears to be important primarily in surmounting the potential energy barrier to reaction; in ion-molecule systems, especially when reagent charge transfer is near resonant, reagent vibration is very important in influencing such effects as charge transfer and surface hopping. In the H_4^+ system the electronic effects induced by vibrational excitation overshadow the effect of enhanced nuclear motion.

Our data has clearly shown the sensitivity of the vibrational dependence of reaction cross sections on the detailed nature of the reaction PES. It has been shown to be a useful probe for understanding multipotential energy effects like surface hopping and charge state mixing. It also has allowed us to examine the competition effects between triatomic ion formation and collision induced dissociation.

By examining the competition between reaction, CID, and charge transfer, we can infer something about the range of impact parameters which contribute to each process. As discussed previously, the large magnitude, collision energy independent cross section for charge transfer (Fig. 7) implies that this is a process which is effective even with a large impact parameter. At very low collision energies, the reaction cross section is quite large, leading to some competition with the charge transfer process which can be seen in Fig. 7. As the collision energy increases, the range of impact parameters leading to reaction becomes smaller, and reaction ceases to compete with CT, although in reactive collisions, CT may still occur at long range in the entrance channel. Above 3 eV the CID process begins to compete with reaction. Although, both processes occur at small impact parameters, comparison of Figs. 3-6 suggest that the competition is very complicated, with strong dependence on collision energy and reagent vibrational state. This again indicates that the competition between product formation and collisional dissociation is not a simple branching of some common intermediates. There must be some basic difference in the nature of collisions leading to the two processes; perhaps orientation, or whether charge transfer occurred in the reaction entrance channel.

Many questions still remain concerning competition between various processes, excited state dynamics, etc. More detailed theoretical investigation will be required before the detailed reaction dynamics will be understood. The H_4^+ system is clearly a useful paradigm for more complex multisurface problems, and the new detailed data available should provide a sensitive test for the development of new theoretical models.

ACKNOWLEDGMENT

This work was supported by the Director, Office of Energy Research, Office of Basic Energy Sciences, Chemical Sciences Division of the U.S. Department of Energy under Contract Number W-7405-ENG-48.

- ¹E. Herbst and W. Klemperer, *Astrophys. J.* **185**, 505 (1973); W. D. Watson, *ibid.* **183**, 117 (1973).
- ²S. S. Prasad and A. Tan, *Geophys. Res. Lett.* **1**, 337 (1979).
- ³J. R. Krenos, K. K. Lehman, J. C. Tully, P. M. Hierl, and G. P. Smith, *Chem. Phys.* **16**, 109 (1976); P. M. Hierl and Z. Herman, *ibid.* **50**, 249 (1980).
- ⁴D. W. Vance and T. L. Bailey, *J. Chem. Phys.* **44**, 486 (1966). J. H. Futrell and F. P. Abramson, *Adv. Chem. Ser.* **58**, 123 (1966).
- ⁵C. H. Douglass, D. J. McClure, and W. R. Gentry, *J. Chem. Phys.* **67**, 4931 (1977).
- ⁶A. B. Lees and P. K. Rol, *J. Chem. Phys.* **61**, 4444 (1974).
- ⁷W. A. Chupka, M. E. Russell, and K. Refaey, *J. Chem. Phys.* **48**, 1518 (1968).
- ⁸W. T. Huntress, D. D. Elleman, and M. T. Bowers, *J. Chem. Phys.* **55**, 5413 (1971).
- ⁹L. D. Doverspike and R. L. Champion, *J. Chem. Phys.* **46**, 4718 (1967).
- ¹⁰S. L. Anderson, T. Hirooka, P. W. Tiedemann, B. H. Mahan, and Y. T. Lee, *J. Chem. Phys.* **73**, 4779 (1980).
- ¹¹J. T. Muckerman (private communication).
- ¹²I. Koyono and K. Tanaka, *J. Chem. Phys.* **72**, 4858 (1980).
- ¹³J. R. Stine and J. T. Muckerman, *J. Chem. Phys.* **68**, 185 (1978).
- ¹⁴S. Sakai, O. Skato, and K. Morokuma, *Ann. Rev. Inst. Mol. Sci. Okazaki, Japan*, 1979; R. F. Borkman and M. Cobb (preprint); M. Cobb, T. F. Moran, R. F. Borkman, and R. Childs, *Chem. Phys. Lett.* **57**, 326 (1978); R. D. Poshusta and D. F. Zetik, *J. Chem. Phys.* **58**, 118 (1973).
- ¹⁵J. A. R. Samson, *J. Electron. Spectrosc. Relat. Phenom.* **8**, 123 (1976).
- ¹⁶W. A. Chupka, in *Ion-Molecule Reactions*, edited by J. Franklin (Plenum, New York, 1972).
- ¹⁷P. M. Dehmer and W. A. Chupka, *J. Chem. Phys.* **65**, 2243 (1976).
- ¹⁸E. Tely and D. Gerlich, *Chem. Phys.* **4**, 417 (1974); D. Gerlich, Diplomarbeit, Fakultät für Physik der Universität Freiburg i/Br, Freiburg, W. Germany (1971).
- ¹⁹P. J. Chantry, *J. Chem. Phys.* **55**, 2746 (1971).
- ²⁰N. R. Daly, *Rev. Sci. Instrum.* **31**, 264 (1960).
- ²¹P. M. Dehmer and W. A. Chupka, *J. Chem. Phys.* **66**, 1972 (1977).
- ²²J. Futrell and F. Abramson, in *Ion Molecule Reactions in the Gas Phase* (ACS, Washington, 1966), p. 123.
- ²³J. Durup and M. Durup, *J. Chem. Phys.* **64**, 386 (1967).